Simulations of Microlens Arrays Formed by Pattern-Photopolymerization-Induced Phase Separation of Liquid Crystal/Monomer Mixtures

Thein Kyu* and Domasius Nwabunma

Institute of Polymer Engineering, The University of Akron, Akron, Ohio 44325-0301

Received April 2, 2001; Revised Manuscript Received August 15, 2001

ABSTRACT: Simulations are presented for microlens arrays prepared via photopolymerization-induced phase separation in liquid crystal/monomer mixtures based on four-wave mixing, viz., interference of two horizontal waves and two vertical waves. The microlens forming process has been simulated on the basis of a pattern-photopolymerization technique in which the spatially modulated reaction rate has been coupled with the time-dependent Ginzburg−Landau (TDGL) equations via incorporation of the free energies pertaining to isotropic mixing, nematic ordering, and network elasticity. The simulation suggests that the LC microlens arrays are similar to compound eyes found in various insects such as flies, ants, and wasps.

Introduction

Liquid crystal (LC)/polymer composites are materials of technological importance in electrooptical displays and control devices.[1] Typical examples include polymer-dispersed liquid crystals (PDLC) for electrical switching and polymer stabilized cholesteric liquid crystals (PSLC) for refractive color display.[1] These LC/polymer composites are customarily formed by polymerization-induced phase separation (PIPS) through thermal and/or photoinitiation in the initially homogeneous state. Recently, this concept has been extended to electrically switchable holographic polymer dispersed liquid crystals (H-PDLC)[2,3] through pattern photopolymerization using two interference UV waves. It was demonstrated experimentally that LC droplets were primarily formed in the low-intensity region created by the constructive and destructive interference of the UV waves, thereby forming stratified layers of the size of a few hundred nanometers.[2,3] Recently, the formation and spatiotemporal growth of the LC domains in the stratified LC layers have been demonstrated theoretically based on the time-dependent Ginzburg−Landau (TDGL), called model C, equations, in which the compositional order parameter and the orientational order parameter of the LC directors are coupled in conjunction with the spatially modulated UV photopolymerization rate.[4]

Another area of interest of the LC materials is the development of microlens because the focal length is electrically tunable, thus having potential for applications such as optical beam steering and image processing.[5,6] The principle of focal length tuning of a microlens is illustrated in Figure 1. In the absence of an external electric field, the LC directors are randomly oriented, causing light to scatter. When a voltage is applied across the LC microdroplet, the LC directors tend to align toward the field direction, e.g., along the droplet curvature near the surface, but tend to become straight near the center. The curvature of the LC alignment may be altered by the electrical field, which in turn guides the incoming light waves to converge to a focal point.

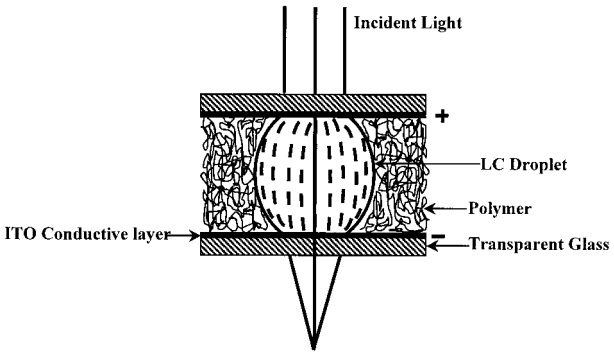

Figure 1. Schematic illustration of the principle of focal length tuning of a microlens.

In this manner, the focal length can be tuned by controlling the applied voltage. The validity of the aforementioned principle of the tunable microlens has been demonstrated experimentally.[5,6]

The LC microlens arrays, hitherto reported,[7−9] have been fabricated by drilling holes on indium−tin oxide (ITO)-coated glass electrodes and then filling them with liquid crystals. Another way of fabricating a microlens is through pattern photopolymerization of LC/photocurable monomer mixtures by either masking with an array of black dots[5,6] or patterning with parallel electrodes. However, these drilled holes, masking dots, or microelectrodes are too large to fabricate microlens of nanosizes; most microlens thus produced are at best in the range of a few hundred micrometers in size. For better image resolution, it is desirable to reduce the microlens size to a few hundred nanometers or smaller, which motivates the present study.

The present paper is a first attempt to fabricate microlens arrays via photopolymerization-induced phase separation of LC/monomer mixtures on the basis of a four-wave mixing technique. This method is basically similar to producing holographic polymer dispersed liquid crystals in which the LC stripes are formed by interference of two planar UV waves, except that the LC microlens are formed by interference of two horizontal waves and two vertical waves. Unlike the conventional methods of making LC microlens, the novel

* To whom correspondence should be addressed. E-mail: tkyu@uakron.edu.

10.1021/ma010567f CCC: $20.00
Published on Web 11/08/2001

four-wave mixing technique affords ease of fabrication (one short patterning process) of microlens arrays in the range of a few hundred nanometers by maneuvering the interference angles of the two horizontal and two vertical UV waves. The LC microlens forming process has been simulated on the basis of a pattern-photopolymerization technique in which the spatially modulated photoreaction rate is coupled with the time dependent Ginzburg−Landau (TDGL) equations (model C) by incorporating free energy densities of isotropic mixing, nematic ordering, and network elasticity.

The aforementioned TDGL approach has been successfully applied to a thermal quench-induced phase separation of a PDLC system in which the emerging morphologies have been analyzed in the context of the curvature gradient coefficients tensors and the coupling coefficient tensors by Lapena et al.[10] The advantage of the tensorial forms is that it is possible to mimic the LC topological defects which is not feasible with the present scalar order parameter approach. However, one drawback of the tensorial approach is that it is impractical to experimentally determine the individual elements of these coefficient tensors of the curvature gradient, particularly those of the coupling coefficients.

For the present purpose, the scalar approach appears adequate in elucidating the emergence of morphology in photoinitiated PIPS of the LC/polymer mixture. The reference LC system under consideration is a single-component nematic, namely 4-*n*-heptyl-4′-cyanobiphenyl (K21), having a nematic−isotropic transition temperature, T_{NI}, of 42 °C, whereas the monomer is a multifunctional UV curable monomer such as NOA65. This LC/monomer mixture was chosen because the temperature vs composition phase diagram of this system was already established in our group.[11,12]

Theoretical Model

The photopatterning process of the LC microlens may be modeled by mimicking spatiotemporal growth of concentration and orientation order parameters of the LC in which a photoreaction rate equation is coupled with the TDGL model C, as described below:[11−14]

$$\frac{\partial \phi_M}{\partial t} = \nabla\cdot\left[\Lambda\nabla\frac{\delta G}{\delta \phi_M}\right] + \eta_{\phi_M} \quad \text{or}$$

$$\frac{\partial \phi_P}{\partial t} = \nabla\cdot\left[\Lambda\nabla\frac{\delta G}{\delta \phi_P}\right] + \eta_{\phi_P} \qquad (1)$$

$$\frac{\partial \phi_L(r,t)}{\partial t} = \nabla\cdot\left[\Lambda\nabla\left(\frac{\delta G}{\delta \phi_L}\right)\right] + \eta_{\phi_L} \qquad (2)$$

$$\frac{\partial s(r,t)}{\partial t} = -R\left(\frac{\delta G}{\delta s}\right) + \eta_S \qquad (3)$$

where $\phi_L(r,t)$ is the conserved concentration (volume fraction) order parameter of LC at position r and time t, whereas $s(r,t)$ is the nonconserved orientational order parameter. The noise terms, $\eta_{\phi_P}(r,t)$ and $\eta_{\phi_L}(r,t)$, represent the concentration fluctuations of polymer and LC, respectively, and $\eta_s(r,t)$ signifies the orientation fluctuations of the LC directors that satisfy the fluctuation−dissipation theorem. If the monomer and polymer were immiscible, it is necessary to solve three-coupled equations, i.e., eqs 1−3; otherwise, only two-coupled equations would be sufficient, e.g., eq 3 with eq 1 or with eq 2. We chose eqs 2 and 3 in the simulation under the assumption that the monomers and the emerging polymer are miscible. Furthermore, the monomer, $\phi_M(r,t)$, and polymer, $\phi_P(r,t)$, concentration are related to $\phi_L(r,t)$ via the fractional conversion, α, viz. $\phi_M = (1 - \alpha)(1 - \phi_L)$ and $\phi_P = \alpha(1 - \phi_L)$, respectively. Since the photopolymerization rate, $d\alpha/dt$, is proportional to the square root of the UV intensity, I_0, it may be represented in the periodic form:

$$\frac{d\alpha}{dt} = k_0 {I_0}^{1/2}\left[\cos\left(\frac{N_x\pi}{L}x\right) + \cos\left(\frac{N_y\pi}{L}y\right)\right](1 - \alpha) \qquad (4)$$

where k_0 is the reaction rate constant. N_x and N_y represent the number of layers, related to the interference angles or periodicity in the horizontal and vertical directions, respectively. L is the size of an assumed square grid. Equation 4 enables the fabrication of microlens arrays of spherical droplets ($N_x = N_y$) or of elliptical shapes ($N_x \neq N_y$). Λ represents the mutual diffusion coefficient having the property of Onsager reciprocity, while R is related to the rotational mobility.[12,13] The quantities η_{ϕ_L} and η_S are thermal noise in the respective concentration and orientation fields, while G is the total free energy of the system, which may be written as[4,12]

$$G = \int_v [g(\phi_L,\phi_M,\phi_P,s) + \kappa_\phi|\nabla\phi_L|^2 + \kappa_s|\nabla s|^2]\, dv \qquad (5)$$

where $g(\phi_L,\phi_M,\phi_P,s)$ or g for brevity is the local free energy density of the system. The terms $\kappa_\phi|\nabla\phi_L|^2$ and $\kappa_s|\nabla s|^2$ are nonlocal terms associated with the gradients of the LC concentration and orientation fluctuations, respectively, while κ_ϕ and κ_s are the corresponding interface gradient coefficients. The local free energy density, g, may be expressed as the sum of the isotropic mixing (g^i), nematic ordering (g^n), and elastic (g^e) free energy densities. The free energy density of isotropic mixing, g^i, may be described in the context of the Flory−Huggins theory extended to a three-component system as follows:[15, 16]

$$g^i = \phi_L \ln \phi_L + \phi_M \ln \phi_M + \chi(\phi_L\phi_M + \phi_L\phi_P) \qquad (6)$$

Equation 6 assumes that the polymer is cross-linked so that the average degree of polymerization, $r_P = \infty$, while segment lengths of LC, r_L, and monomer, r_M, are each taken as unity. It is also assumed that the monomer is miscible with polymer so that the monomer−polymer interaction parameter, χ_{MP}, may be taken as zero, while LC−monomer and LC−polymer interaction parameters χ_{LM} and χ_{LP}, respectively, are assumed equal to χ.[11] The nematic ordering free energy density, g^n, is given by the Maier−Saupe theory:[17]

$$g^n = \frac{1}{r_L}\left(-\phi_L \ln z + \frac{1}{2}\nu{\phi_L}^2 s^2\right) \qquad (7)$$

where ν is the nematic interaction parameter related to the T_{NI}, while z and s are respectively the partition function and the orientational order parameter.[17] The elastic free energy, g^e, for a cross-linked polymer is given according to Dusek's approach:[18]

$$g^e = \frac{3\alpha_e}{2r_c}{\Phi_0}^{2/3}({\phi_P}^{1/3} - \phi_P) + \frac{\beta_e}{r_c}\phi_P \ln \phi_P \qquad (8)$$

where r_c is segment length between cross-linked point,

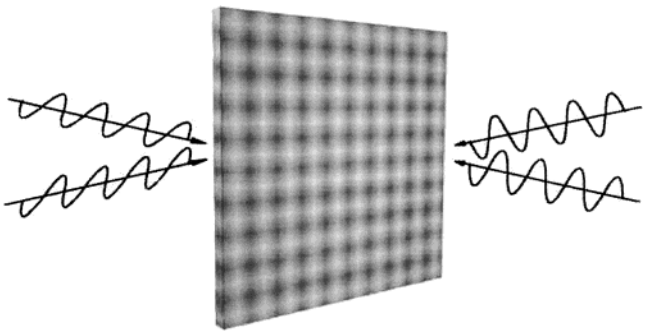

Figure 2. Schematic illustration of a fabricating process of a LC microlens via pattern photopolymerization based on four-wave mixing.

while α_e and β_e are network model constants (see refs 11 and 12). The parameter F_0 in eq 8 is the reference volume fraction of the network, which gives $F_0 = \phi_P$ for in-situ cross-linking (the volume fraction at the onset of cross-linking).[12]

Equations 2 and 3 have been solved numerically using a finite difference method on a 128 × 128 square grid under specified initial boundary conditions. For the spatial step, the Euler's central difference discretization scheme was used, whereas an explicit forward difference discretization was utilized for the temporal step along with a periodic boundary condition. Prior to the simulation, the initial LC volume fractions, $\phi_L(r,0)$, at grid points was calculated by adding random thermal noise satisfying the fluctuation dissipation theorem, and then $s(r,0)$ were determined from the known $\phi_L(r,0)$. By marching forward in time, values of $\phi_L(r,t)$ and $s(r,t)$ at all grid points were computed. It should be emphasized that both the grid spacing and the time step increments were maintained at values that were sufficiently small to ensure that changes in them exerted little or no influence on the results. Moreover, a few preliminary simulations were carried out using a more complicated implicit method with similar grid sizes and time steps in order to determine whether the results depended on the simulation scheme.

Results and Discussion

Figure 2 exhibits a schematic diagram of the four-wave mixing technique for fabricating LC microlens in which two waves are mixed to form interference striations in the horizontal direction while the other two waves generate interference striations in the vertical direction. The horizontal and vertical striations are then impinged on the sample to generate droplet array patterns in the sample plane. Alternatively, these four waves may be applied from one side of the film so long as the stratified layers created by the interference are orthogonal to each other. If the film has some finite thickness, a six-wave mixing method may be utilized by applying two additional interference waves in the thickness direction. This six-wave method is reserved for a future publication, and thus it will not be disclosed in the present paper. It can be anticipated that polymerization occurs preferentially in the high-intensity regions due to the fast photoreaction rate that makes LC molecules diffuse into the low-intensity regions and form droplets. As the size of the LC domains is controllable by maneuvering the interference angles of the waves, a uniform array of microlens may be obtained.

Figure 3 demonstrates the time sequence of the spatiotemporal development of microlens arrays calculated using the parameters: $\phi_L = 0.75$, $T = 30$ °C, $k_0 = 10^{-4}$, $I_0 = 1$, $N_x = N_y = 16$. The upper row shows the emerging patterns in the compositional order parameter field, while the lower row represents those in the orientational order parameter field. Note that the reaction temperature of 30 °C corresponds to the

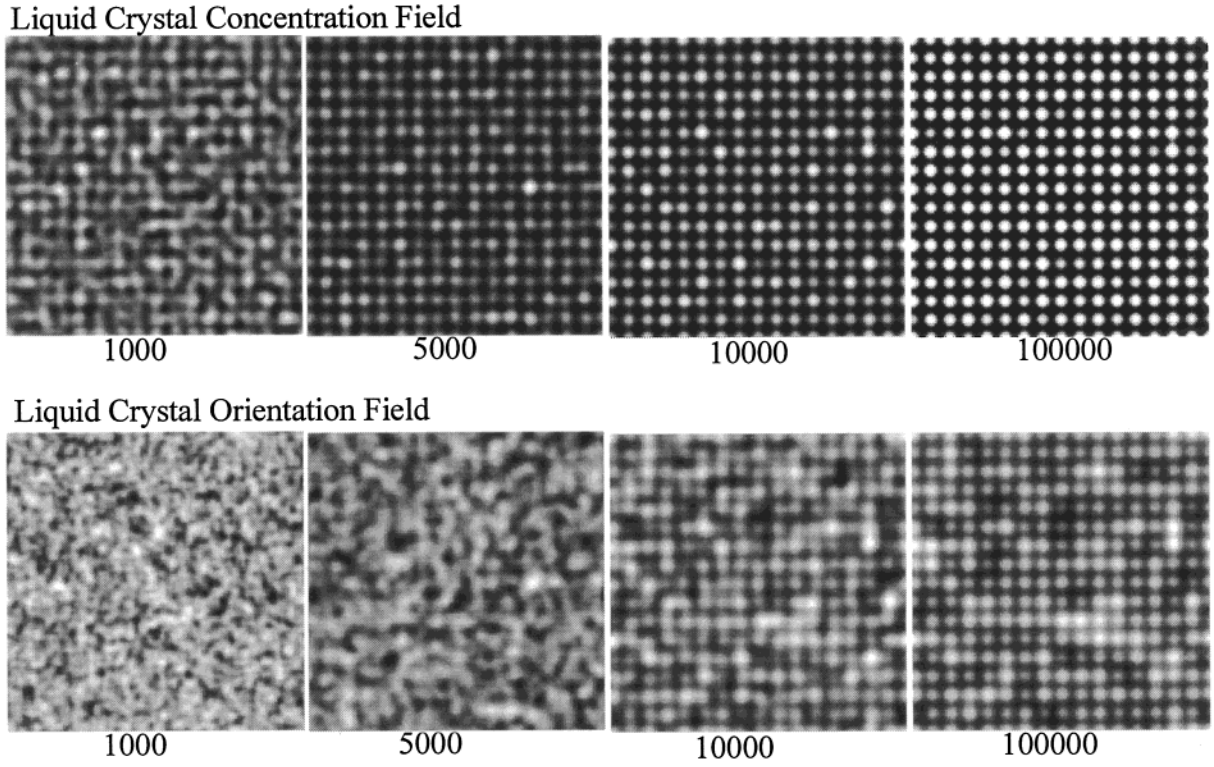

Figure 3. Snapshots of the emergence of a hypothetical LC microlens showing droplet array patterns. Parameters used were $\phi_L = 0.75$, $T = 30$ °C, $k_0 = 10^{-4}$, $I_0 = 1$, and $N_x = N_y = 16$.

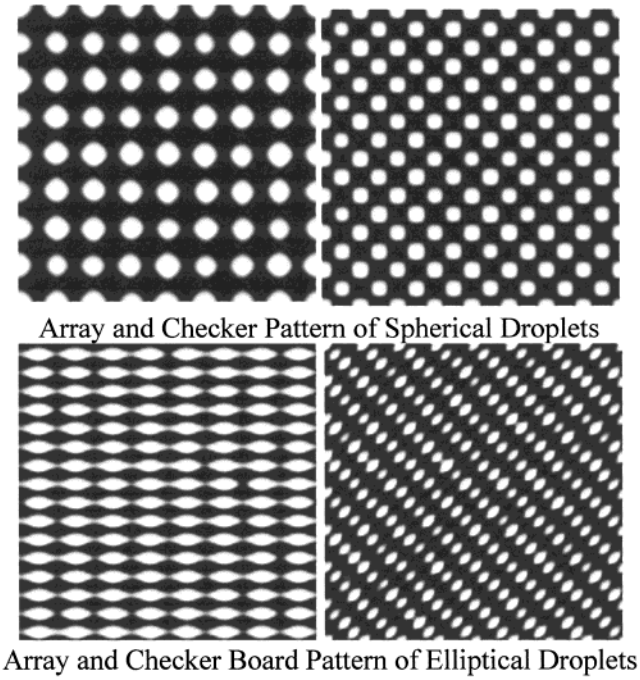

Figure 4. Various simulated morphological topologies of LC microlens with spherical and elliptical droplets arranged in an array (upper left) or a checker board (upper right) pattern and the corresponding elliptical droplets (lower row). The parameters used were $N_x = N_y = 8$ for the spherical droplets (upper row) and $N_x = 16$ and $N_y = 8$ for the elliptical droplets (lower row). The dimensionless time step is 10^5 in all cases.

isotropic state of the starting LC/monomer mixture (see Figure 1 of ref 11). The domain pattern in the concentration order parameter field that emerged from the pattern-photopolymerization-induced phase separation (1000 steps) appears connected initially. With elapsed time, the spherical LC droplets eventually arrange themselves in the form of droplet arrays (10^4-10^5 time steps). The LC ordering seemingly lags behind that of the compositional order parameter, showing a spinodal-like modulated pattern initially, but the texture eventually evolves into the droplet arrays at later times. It should be noted in the simulation that only LC and monomer are allowed to diffuse mutually, while the polymer (dark background in Figure 2) is virtually fixed due to the network formation.

In the simulation, one can envisage the emergence of microlens with varying shapes, viz., spherical or elliptical as depicted in Figure 4. As seen in the upper left figure, the interference of two vertical waves gives rise to the array of spherical microlens when $N_x = N_y = 8$. However, when the two sets of these interference waves were applied in the diagonal direction, a checkerboard pattern may be generated (upper right). If the interference angle (or the wavelength) of the horizontal waves is different from those of the vertical waves, say $N_x = 16$, $N_y = 8$, the elliptical microlens arrays (lower row) may be obtained. Strictly speaking, the microlens with different shapes were obtained by modulating the interference angle of the UV waves because the orientational order parameter was used as a scalar. One may suspect that if one maintains the tensorial form of the orientational order parameter, it may be possible to get the ellipsoidal droplets after the spinodal decomposition of an ordinary LC mixture. However, it should be pointed out that the ellipsoidal droplet could be obtained even in a non-LC system (e.g., isotropic nonvolatile solvent and UV monomer mixture) where the orientational order parameter is not involved.

As is well-known, the size of the microlens depends on the choice of the characteristic length scale, the characteristic time, and the mutual diffusion coefficient. Assuming the diffusivity to be 10^{-6} cm^2/s (for monomer and/or low molecular weight LC) and the characteristic time for H-PDLC to be 0.0001 s, then the estimated characteristic size would be of the order of 0.1 μm. Hence, the calculated picture frame (128 $\times$ 128) would be approximately 12.8 μm; so the estimated size (diameter) of the microlens would be about 800 nm. Although the estimated size is larger than the reported experimental value of 300 nm for an H-PDLC,[2,3] it is much smaller than the size (a few hundred micrometers) reported for the existing microlens fabricated via other methods.[6−9]

With appropriate configurations of the holographic optics, the size and shape of the LC microlens may be varied through control of the interference angles and/or UV wavelengths, the reaction rate as determined by the incident UV intensity and/or the pattern profiles. It should be emphasized that the focal length of the LC microlens may be tuned by maneuvering the orientation of LC directors through appropriate applied voltage. The electrically focusable microlens are particularly useful when the object being imaged is not in a fixed position. Another important feature is that flexible ITO-coated polymeric films may be used to arrange the arrays of the LC microlens in the convex shape so that these LC microlens would be similar to the compound lens found in the eyes of some insects such as flies, ants, and/or wasps.

In summary, we have demonstrated the feasibility of fabricating electrically tunable LC microlens via photopolymerization-induced phase separation of LC/monomer mixtures using four-wave mixing based on the time-dependent Ginzburg−Landau (TDGL) equations coupled with a spatially modulated photopolymerization rate equation. Simulated results showed that, depending on the interference angles or the periodicity (wavelengths) of the horizontal and vertical waves, it is possible to produce the LC microlens arrays having the spherical (or elliptical) droplet arrays or the checkerboard patterns.

Acknowledgment. This work was made possible through financially support of the NSF-STC Center for Advanced Liquid Crystal Optical Materials (ALCOM): Grant 89-20147, NSF DMR 99-03519, the Ohio Board of Regents (OBR) Research Challenge Grant, and WPAF/TMCI Grant.

References and Notes

(1) Doane, J. W. In *Liquid Crystals: Applications and Uses*; Bahadur, B., Ed.; World Scientific: Singapore, 1991.
(2) Sutherland, R. L.; Tondiglia, V. P.; Natarajan, L. V.; Bunning, T. J.; Wade, W. W. *Appl. Phys. Lett.* **1994**, *64*, 1074.
(3) Tondiglia, V. P.; Natarajan, L. V.; Sutherland, R. L.; Bunning, T. J.; Wade, W. W. *Opt. Lett.* **1995**, *20*, 1325.
(4) Kyu, T.; Nwabunma, D.; Chiu, H.-W. *Phys. Rev. E* **2001**, *63*, 1802.
(5) Nose, T.; Masuda, S.; Sato, S.; Li, J.; Chien, L.-C.; Bos, P. J. *Opt. Lett.* **1997**, *22*, 351.
(6) Nose, T.; Masuda, S.; Sato, S. *Jpn. J. Appl. Phys.* **1992**, *31*, 1643; *Appl. Opt.* **1997**, *37*, 2067.
(7) Williams, G.; Powell, N.; Purvis, A.; Clark, M. G. *SPIE* **1989**, *1168*, 352.
(8) Stalder, M.; Ehberts, P. *Opt. Lett.* **1994**, *19*, 1.
(9) Tam, E. C. *Opt. Lett.* **1992**, *17*, 369.

(10) Lapena, A. M.; Glotzer, S. C.; Langer, S. A.; Liu, A. J. *Phys. Rev. E* **1999**, *60*, 29.
(11) Nwabunma, D.; Kyu, T. *Macromolecules* **1999**, *32*, 664.
(12) Nwabunma, D.; Chiu, H.-W.; Kyu, T. *J. Chem. Phys.* **2000**, *113*, 6429.
(13) Gunton, J. D.; San Miguel, M.; Sahni, P. S. In *Phase Transition and Critical Phenomena*; Domb, D. C., Lebowitz, J. L., Eds.; Academic Press: New York, 1983.
(14) Dorgan, J. R.; Yan, D. *Macromolecules* **1998**, *31*, 193.
(15) Flory, P. J. *J. Chem. Phys.* **1941**, *10*, 51.
(16) Huggins, M. L. *J. Chem. Phys.* **1941**, *9*, 440.
(17) Maier, W.; Saupe, A. *Z. Naturforsch.* **1958**, *A13*, 564; **1959**, *A14*, 882.
(18) Dusek, K. *J. Polym. Sci., Part C* **1967**, *16*, 1289.

MA010567F